

### 3D Acquisition of the Inhomogeneous Magnetization Transfer Effect for Greater White Matter Contrast

Gopal Varma<sup>1</sup>, Gottfried Schlaug<sup>2</sup>, and David C Alsop<sup>1</sup>

<sup>1</sup>Radiology, Division of MR Research, Beth Israel Deaconess Medical Center, Harvard Medical School, Boston, MA, United States, <sup>2</sup>Neurology, Beth Israel Deaconess Medical Center, Harvard Medical School, Boston, MA, United States

**Introduction** The contrast from magnetization transfer (MT) has been extensively explored and in reference to the brain associated with degenerative and neuropsychiatric disease [1-2]. This relationship is based on the bulk MT effect in white matter (WM) being considered to arise from myelin-associated lipids. However the contrast, or MT ratio (MTR) used in most analysis, shows relatively little difference between WM and grey matter (GM), which contains fewer myelinated axons. The bound pool associated with myelin, and its broad line-width, has also been characterized by  $T_2$  mapping [3]. Although extraction of the short  $T_2$  component appears more specific to WM, acquisition of multiple echoes for multi-exponential analysis is time restrictive. Recently, a 2D imaging technique associated with inhomogeneous broadening, inhomogeneous MT (IHMT) showed a contrast more specific to WM [4]. This increased specificity is associated with myelin, in particular the multiple phospholipid bilayers that make up its sheath. Inhomogeneous broadening in bilayers has been attributed to motional restriction of their constituent hydrocarbon chains [5-6]. The IHMT method exploits an inhomogeneously broadened line being made up from packets of spins at different frequencies that do not undergo rapid exchange, by saturation at two opposite frequencies far from resonance. In the case of homogeneous broadening, the result of saturation at a positive or negative offset (Fig.1a) is expected to be equal to that following saturation at both frequencies (Fig.1b). Thus IHMT is elucidated by a difference between saturation independently, when compared with that applied at both offsets. In prior work, IHMT was imaged in a single 2D slice with an MT preparation. Here we report a 3D steady state acquisition approach more similar to traditional MT acquisitions [7].

**Methods** Data were acquired on a 3T GE scanner using an 8-channel head coil. The 3D acquisitions were based on the spoiled gradient-echo (SPGR) sequence with a MT module applied within each TR (Fig.1a): Four experiments made up the total IHMT technique, each with a different saturation module: In the first and third case, a trapezoidal pulse of duration 5ms and  $B_{1,peak}=50mG$  was applied at offsets of +5kHz (P) and -5kHz (N) prior to the SPGR, independently. Second and fourthly, a cosine modulated trapezoidal pulse was employed with  $B_{1,peak}=(\sqrt{2})50mG$  on-resonance (D). An IHMT image, and consequently ratio (IHMTR), was formed by P+N-2D divided by an unsaturated acquisition. Each set of four was acquired thrice for a total acquisition time of ~5mins with: FA=10°; FOV=25x25x16cm<sup>3</sup>; matrix=96x96x60; TE/TR=2/12ms. IHMT datasets from 13 volunteers were acquired and analysed. MTR images were calculated based on saturation at the positive offset (i.e. +5kHz). Regions of interest (ROIs) were drawn in WM: splenium of the corpus callosum (CCspl); genu of corpus callosum (CCge); left and right anterior periventricular areas (antPVL and antPVR); and basal ganglia (BG) GM: left and right putamen (putL and putR); left and right caudate (cauL and cauR) [7].

**Results and Discussion** Figure 2 shows the 3D IHMT data, the images from which can still be used to form MTR images. Reformatting of the 3D data shows a consistent, more pronounced WM contrast from IHMT, up to the cerebellum. The WM/BG GM ratio is greater in the IHMTR, and the IHMTR values within ROIs correlate with those from MTR.

**Conclusions** A 3D IHMT sequence has been developed and applied in vivo. Images show a greater contrast from WM than MT. The IHMTR may be more specific to myelin and thus provide interesting results in application to related pathology.

**References:** [1] Filippi et al. Ann Neurol 43(1998)809-14; [2] Bruno et al. Brain 127(2004)2433-40; [3] MacKay et al. MRM 31(1994)673-7; [4] Alsop et al. Proc Intl Soc Mag Reson Med 12(2004)2324; [5] Chan et al. Nature 231(1971)110-2 [6] Seiter et al. JACS 95(1973)7541-53 [7] Cercignani et al. Neuroimage 31(2006)181-6

ROI	MTR [%]	IHMTR [%]
CCspl	35.4 ± 0.2	6.9 ± 0.2
CCge	33.5 ± 0.2	5.4 ± 0.1
antPVL	31.3 ± 0.2	5.6 ± 0.1
antPVR	31.4 ± 0.2	5.3 ± 0.1
putL	23.5 ± 0.2	3.1 ± 0.1
putR	23.8 ± 0.2	3.0 ± 0.1
cauL	23.6 ± 0.6	3.1 ± 0.3
cauR	23.3 ± 0.5	3.3 ± 0.3
WM	32.9 ± 0.1	5.8 ± 0.1
BG GM	23.6 ± 0.3	3.1 ± 0.2

Table 1 MTR and IHMTR values from ROIs.

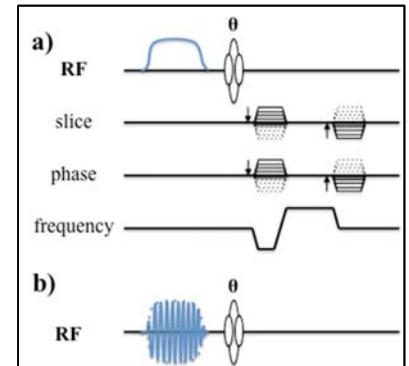


Figure 1 a) SPGR sequence with MT saturation pulse for cases (P) and (N). b) Sinusoid modulated pulse at 0Hz for (D).

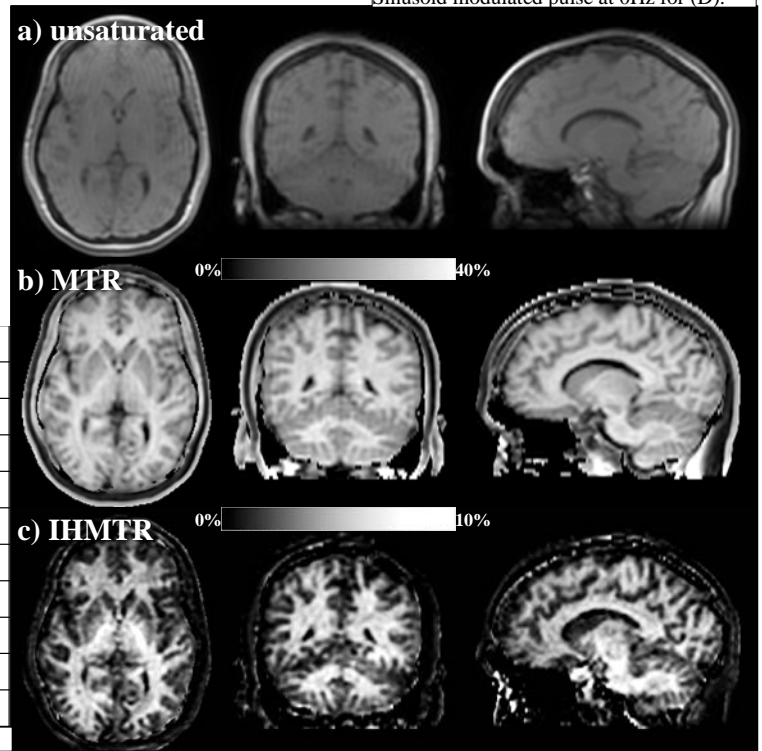


Figure 2 a) unsaturated, b) MTR and c) IHMTR images, displayed in axial orientation and reformatted to show coronal and sagittal views in the middle and right columns.